

Oscillons in coupled Bose-Einstein condensatesShih-Wei Su,¹ Shih-Chuan Gou,¹ I-Kang Liu,¹ Ashton S. Bradley,² Oleksandr Fialko,³ and Joachim Brand⁴¹*Department of Physics and Graduate Institute of Photonics, National Changhua University of Education, Changhua 50058, Taiwan*²*Dodd-Walls Centre for Photonics and Quantum Technology, Department of Physics, University of Otago, Dunedin, New Zealand*³*Centre for Theoretical Chemistry and Physics, Institute for Natural and Mathematical Sciences, Massey University, Auckland, New Zealand*⁴*Dodd-Walls Centre for Photonics and Quantum Technology and Centre for Theoretical Chemistry and Physics, New Zealand Institute for Advanced Study, Massey University, Auckland, New Zealand*

(Received 22 December 2014; published 27 February 2015)

Long-lived, spatially localized, and temporally oscillating nonlinear excitations are predicted by numerical simulation of coupled Gross-Pitaevskii equations. These oscillons closely resemble the time-periodic breather solutions of the sine-Gordon equation but decay slowly by radiating Bogoliubov phonons. Their time-dependent profile is closely matched with solutions of the sine-Gordon equation, which emerges as an effective field theory for the relative phase of two linearly coupled Bose fields in the weak-coupling limit. For strong coupling the long-lived oscillons persist and involve both relative and total phase fields. The oscillons decay via Bogoliubov phonon radiation that is increasingly suppressed for decreasing oscillon amplitude. Possibilities for creating oscillons are addressed in atomic gas experiments by collision of oppositely charged Bose-Josephson vortices and direct phase imprinting.

DOI: [10.1103/PhysRevA.91.023631](https://doi.org/10.1103/PhysRevA.91.023631)

PACS number(s): 03.75.Kk, 03.75.Lm, 05.45.Yv

I. INTRODUCTION

Oscillons are localized and oscillating concentrations of energy in a nonlinear field that decay very slowly over many of their oscillation periods [1–3]. They are thought to be relevant in the dynamics of cosmological phase transitions [4] and inflation scenarios [5], where they provide localized stores of energy. In contrast to cosmic strings [6] or other topological defects that can only be destroyed by annihilation, isolated oscillons can decay by radiation over long time scales. Closely related to oscillons are breathers, which are time-periodic localized solutions of a nonlinear field equation [3]. Breathers only exist when resonance between the breather frequency and extended linear waves is avoided. This is known to happen only in integrable nonlinear wave equations like the sine-Gordon (SG) equation [7] and the nonlinear Schrödinger equation [8], or in nonlinear lattices [9] due to the occurrence of band gaps in the linear wave spectrum. Oscillons are thus the more generic localized and oscillating nonlinear excitations.

In most nonlinear field equations, oscillon solutions are not known in closed form and the investigation of oscillon properties relies on numerical simulations. However, due to the integrability of SG equation in 1 + 1 dimensions [10,11], the closed form solutions of SG breathers as well as solitons can be derived [12]. The fundamental solitons of the SG equation are localized topological excitations with a topological charge of ± 1 known as kinks and antikinks, respectively. Sine-Gordon breathers are localized in space and periodic in time and can be understood as the bound states of kink and antikink. Since their total topological charge is zero, breathers are not protected by their topological properties but rather by the integrable nature of the SG equation. Slight modifications of the equation that break the integrability typically destroy the breather solutions. However, numerical methods can still find long-lived spatially localized and oscillating concentrations of energy, namely, oscillons [3,13,14].

Linearly coupled BECs have been proposed as a model system to simulate the sine-Gordon equation in a variety of

contexts [15–17]. This has aroused considerable interest in investigating the excitations of linearly coupled Bose gases, in particular Josephson vortices, which are closely related to SG kinks [18–22]. In a recent paper several of us simulated the spontaneous formation and decay of Josephson vortices within the Kibble-Zurek scenario of a rapid quench through the BEC phase transition in quasi-one-dimensional coupled Bose gases [23]. The finding that post-quench dynamics and in particular the collision and annihilation of Josephson vortices contribute decisively to the breakdown of Kibble-Zurek scaling laws has motivated the current study. As shown in Sec. IV A, the collision of slow and oppositely charged Josephson vortices generically produces oscillons.

It has further been suggested that breather-like excitations (oscillons) with a finite lifetime can be spontaneously formed in coupled BECs via a dynamical instability triggered by parametric amplification of quantum fluctuations [16]. This emergence of localized excitations from amplified quantum fluctuations bears close analogy with the formation of oscillons after inflation of the early universe predicted within relativistic cosmological models [5]. The coupled BECs may thus provide an experimentally accessible model to simulate the evolution of the early universe [17].

While recent works on simulating the SG model using coupled BECs have focused entirely on the relative phase dynamics [15–17], this picture neglects the coupling to the symmetric degrees of freedom in the system, such as the total phase and densities of the condensates. Realistically, such couplings can serve as channels of decoherence that can significantly alter the relative-phase dynamics and then lead to the instability of nontopological excitations, such as breathers. A similar circumstance arises, for example, in annular Josephson junctions, where an effective dissipation is introduced by carefully eliminating electronic degrees of freedom [24,25]. By the same token, it has been shown that the breathers are not robust against an ambient perturbation and hence decay by continuously radiating phonons [26–28] thus forming oscillons. This motivates us to carry out a detailed

study of the full dynamics of breather-like excitations in BECs. Specifically, we investigate the time evolution of an initial SG breather state by numerically solving the Gross-Pitaevskii equation over broad ranges of coupling energy and imprinted SG breather frequency. We assess the stability of the long-lived oscillon, and present a simple and feasible experimental scheme to create an oscillon by the phase-imprinting method in a double-ring BEC system.

The organization of this paper is as follows. In Sec. II, we give a brief account of the system consisting of two linearly coupled BECs. We outline the emergent SG sector in the weak-coupling limit, and its kink solutions. In Sec. III, we numerically demonstrate that the oscillon forms by imprinting the SG breather onto the initial state of the BECs, and the stability of the oscillon is studied for broad ranges of coupling energy and imprinted SG breather frequency. In Sec. IV, we demonstrate the creation of an oscillon from the collision of two Josephson vortices, and outline experimental constraints for a realistic phase-imprinting protocol in a double-ring geometry. We conclude in Sec. V.

II. MODEL

We consider a system consisting of two linearly coupled BECs, which are tightly confined in the transverse directions but loosely confined in the longitudinal direction. The grand-canonical Gross-Pitaevskii (GP) energy functional for this quasi-one-dimensional system is given by

$$E = \sum_{j=1,2} \int dz \left[\frac{\hbar^2}{2m} |\partial_z \psi_j(z)|^2 + \frac{g}{2} |\psi_j(z)|^4 - \mu |\psi_j|^2 \right] - \tilde{v} \int dz [\psi_1^*(z) \psi_2(z) + \psi_2^*(z) \psi_1(z)], \quad (1)$$

where ψ_j is the order parameter of the j th condensate, μ the chemical potential, \tilde{v} the coupling strength characterizing the tunneling energy between the two systems, and g the effective nonlinear interaction strength. The equation of motion for each ψ_j can be derived via the Hartree variational principle, namely, $i\hbar\partial_t \psi_j = \delta E / \delta \psi_j^*$. For computational simplicity, we let the length and time to be scaled in units of $l_c = \hbar / \sqrt{m\mu}$ and $t_0 = \hbar / \mu$, respectively, so that the coupled GP equations are expressed in the dimensionless form

$$\begin{aligned} i\partial_t \psi_1 &= (-\partial_z^2/2 + |\psi_1|^2 - 1)\psi_1 - \nu\psi_2, \\ i\partial_t \psi_2 &= (-\partial_z^2/2 + |\psi_2|^2 - 1)\psi_2 - \nu\psi_1, \end{aligned} \quad (2)$$

where $\nu = \tilde{v}/\mu$ is the dimensionless coupling energy.

The ground state of the coupled BECs can be determined by minimizing the energy functional, Eq. (1), where we seek the minimum of $V(\psi_1, \psi_2) \equiv \sum_{j=1,2} \int |\psi_j|^2 [\frac{1}{2} |\psi_j|^2 - 1] - \nu[\psi_1^* \psi_2 + \psi_2^* \psi_1]$. The symmetry $V(\psi_1, \psi_2) = V(\psi_2, \psi_1)$ imposes a common amplitude for the ground-state fields. Taking $\psi_1^0 = \sqrt{\rho_0} e^{i\phi_1}$, $\psi_2^0 = \sqrt{\rho_0} e^{i\phi_2}$, and $\Delta = \phi_1 - \phi_2$, the minimum of $V = \rho_0^2 - 2\mu\rho_0 - 2\nu\rho_0 \cos \Delta$ occurs at $\Delta = 0$ and $\rho_0 = (1 + \nu)$.

A. Collective excitations

To find the low-lying excitations above the ground state, we can replace ψ_j with $\psi_j^0 + \alpha_q^j e^{iqz - i\omega t} - \beta_q^{j*} e^{-iqz + i\omega t}$ in Eq. (2) and retain the expressions up to the linear order in α_q and β_q , which then leads to the Bogoliubov-de Gennes (BdG) equation

$$\begin{bmatrix} H_0 - \omega & -(1 + \nu) & -\nu & 0 \\ 1 + \nu & -H_0 - \omega & 0 & \nu \\ -\nu & 0 & H_0 - \omega & -(1 + \nu) \\ 0 & \nu & 1 + \nu & -H_0 - \omega \end{bmatrix} \times \begin{bmatrix} \alpha_q^1 \\ \beta_q^1 \\ \alpha_q^2 \\ \beta_q^2 \end{bmatrix} = 0, \quad (3)$$

where $H_0 = q^2/2 + (1 + 2\nu)$. The low-lying excitation spectrum is determined by solving the eigenvalue problem, Eq. (3). As a result, we obtain two distinct dispersion relations for the excited modes:

$$\omega_1 = \sqrt{\frac{q^2}{2} \left(\frac{q^2}{2} + 2\nu + 2 \right)}, \quad (4)$$

with the eigenvector $\sim (u, v, u, v)^T$, and

$$\omega_2 = \sqrt{\left(\frac{q^2}{2} + 2\nu \right) \left(\frac{q^2}{2} + 4\nu + 2 \right)}, \quad (5)$$

with the eigenvector $\sim (u, -v, -u, v)^T$. Equation (4) represents a gapless mode, corresponding to the in-phase excitation of the two components of condensates, which manifests itself as the Bogoliubov sound wave propagating at a speed $v_{\text{Bog}} = \sqrt{1 + \nu}$. On the other hand, Eq. (5) indicates a gapped mode, which corresponds to out-of-phase excitation. It should be noted that these two modes are decoupled in the linear approximation. Moreover, the gapped excitation possesses a relativistic energy dispersion $\omega_2^2 = q^2 c_2^2 + m_2^2 c_2^4$ with sound speed, $c_2^2 = 1 + 3\nu$ and the rest energy, $m_2^2 c_2^4 = 4\nu(1 + 2\nu)$. The gapless branch accounts for the relative phase dynamics which can be described by the sine-Gordon equation [17].

B. Sine-Gordon regime

Before studying the oscillon excitation in linearly coupled BECs, we investigate the low-energy dynamics of the symmetric degrees of freedom. In general, the order parameters of the coupled BECs can be represented by $\psi_1 = \sqrt{\rho} e^{i(\phi_s + \phi_a)/2} \sin \theta$ and $\psi_2 = \sqrt{\rho} e^{i(\phi_s - \phi_a)/2} \cos \theta$, where ϕ_s and ϕ_a are, respectively, the total and relative phase, ρ the total density, and θ is the density mixing angle. Substituting ψ_1 and ψ_2 into Eq. (1) with the assumption that the coupling between the two BECs is sufficiently weak, and following the arguments used in Ref. [17], we obtain the relevant Hamiltonian density accounting for the sine-Gordon dynamics

$$\begin{aligned} H_{\text{SG}} &= \frac{(1 + \nu)}{4} (\partial_z \phi_a)^2 + (1 + \nu)^2 (1 + \cos 4\theta) \\ &\quad - 2\nu(1 + \nu) (\cos \phi_a - 1) \sin 2\theta, \end{aligned} \quad (6)$$

where the total density ρ is replaced by the sum of the ground-state density of the two components, namely, $2\rho_0 = 2(1 + \nu)$. Using the variational principle, the Euler-Lagrange equation of the relative phase is derived [17],

$$\partial_t^2 \phi_a - (1 + \nu) \partial_z^2 \phi_a + 4\nu(1 + \nu) \sin \phi_a = 0, \quad (7)$$

which is equivalent to the SG equation. It is well known that the SG equation possesses the topologically protected kink and antikink solutions [12], i.e.,

$$\phi_a^S = 4 \tan^{-1} \left[\exp \left(\pm \sqrt{4\nu} \frac{z - z_0}{\sqrt{1 - 2\nu^2/(1 + \nu)}} \right) \right], \quad (8)$$

where the $+$ ($-$) sign corresponds to the kink (antikink) and ν and z_0 are the velocity and the initial location of the (anti)kink, respectively. Remarkably, the kink and antikink in Eq. (8) may form a bound kink-antikink pair. Such a solution does exist for the SG model, which is spatially localized but temporally oscillating, and is thus called breather,

$$\phi_a^B = 4 \tan^{-1} \left[\frac{\sqrt{1 + \nu} \sin \sqrt{\frac{4\nu}{1 + u^2/(1 + \nu)}} ut}{u \cosh \sqrt{\frac{4\nu}{1 + u^2/(1 + \nu)}} z} \right]. \quad (9)$$

Here u is a positive constant that parametrizes the amplitude and frequency of the breather by

$$\phi_{a,\max}^B = 4 \tan^{-1} \left(\frac{\sqrt{1 + \nu}}{u} \right), \quad (10)$$

and

$$\omega_B = u \sqrt{\frac{4\nu}{1 + \frac{u^2}{1 + \nu}}}, \quad (11)$$

respectively. In contrast to kink and antikink, the breather is not protected by topology but is protected by the integrability of the SG equation. The breather becomes unstable once the integrability is broken. From Eq. (9), we can define the full width at half maximum (FWHM) of the breather, $z_w = \sqrt{[1 + u^2/(1 + \nu)]/4\nu} \operatorname{sech}^{-1}(1/2)$. Note that the amplitude (frequency) decreases (increases) with increasing u . With Eq. (9), it is straightforward to show that the energy of a breather is given by

$$E_B = 16(1 + \nu) \sqrt{\nu(1 - \tilde{\omega}^2)}, \quad (12)$$

with $\tilde{\omega} = \omega_B/\sqrt{4\nu(1 + \nu)}$ [29]. In addition to the kink and breather, the SG equation also possesses extended phonon excitations [12].

The Hamiltonian, Eq. (6), represents an emergent SG sector in the weak coupling limit of the total GP Hamiltonian, where the latter supports excitations described by both asymmetric and symmetric degrees of freedom. Excitations in the SG sector such as the kink, breather, and phonon depend only on the asymmetric degrees of freedom. On the other hand, off the SG sector, there are other types of excitations depending on the symmetric degrees of freedom, such as the Bogoliubov phonon (gapless excitation) and the GP dark (grey) soliton which has a 2π ($<2\pi$) phase jump in the total phase. Under the framework of the full GP formalism, these excitations of different degrees of freedoms would couple to each other and these couplings would play an important role in the dynamics of

the condensates. Therefore, it is expected that the SG breather is not stable in the presence of these couplings and would decay by slowly radiating energy, thus forming a so-called oscillon. In the following section, we investigate dynamics of the oscillon excitations in the linearly coupled BECs.

III. DYNAMICAL STABILITY

To create an oscillon, we begin with a phase-imprinted SG breather, with the relative phase given by Eq. (9), initially imprinted into a system of two linearly coupled BECs in a double-ring geometry. The couplings between different degrees of freedom lead to the instability of the initially imprinted breather and result in energy radiation in terms of sound waves. We expect that the propagation of the emitted sound waves may introduce extra effects to the dynamics of the oscillon, and our aim is to investigate how the oscillon evolves under the influence of the evolving background condensates.

A technical issue arises, namely, that since we impose periodic boundary conditions corresponding to a double-ring geometry for the numerical computations, whenever the outgoing sound waves reach one of the boundaries they will re-enter the system from the boundary at the opposite side. These re-entering waves will interfere with those outgoing ones and also interact with the oscillon, complicating the dynamics in an uncontrollable way. To suppress the reentry of the emitted sound waves, we impose the absorption boundary layers by including a position-dependent damping coefficient $\sigma(z)$ in Eq. (2), which turns Eq. (2) into a damped GP equation [30–32]

$$i \partial_t \psi_1 = (1 - i\sigma) [(-\partial_z^2/2 + |\psi_1|^2 - 1)\psi_1 - \nu\psi_2], \quad (13)$$

$$i \partial_t \psi_2 = (1 - i\sigma) [(-\partial_z^2/2 + |\psi_2|^2 - 1)\psi_2 - \nu\psi_1]. \quad (14)$$

The damping coefficient σ varies with z according to the prescription $\sigma(z) = 1 + [\operatorname{erf}(s(z - z_0)) - \operatorname{erf}(s(z + z_0))]/2$, where z_0 and $1/s$ are the center and the width of the error function, respectively. In the simulations, z_0 is chosen to be located far from the origin and s is set to be sufficiently small, such that σ is increasing smoothly over the boundary layer and the reflected sound waves are greatly reduced. From a physical point of view, the absorber means that we are effectively considering a very large ring system, where the feedback from acoustic emissions lags the oscillon dynamics by a significant time scale.

In what follows, we present the main results obtained by numerically integrating Eqs. (13) and (14) over a variety of initial conditions, where the space integration is by the highly accurate Fourier pseudospectral method, and the time integration is by the adaptive Runge-Kutta method of orders 4 and 5 (RK45).

A. Dynamics of the oscillon

To study the dynamics and stability of oscillons in the coupled BECs, we imprint the phase profile of the SG breather, ϕ_a^B , which is defined in Eq. (9), onto the homogeneous background density $n_1^0 = n_2^0 = 1 + \nu$,

$$\psi_1(t = 0) = \psi_2^*(t = 0) = \sqrt{1 + \nu} e^{i\phi_a^B/2}, \quad (15)$$

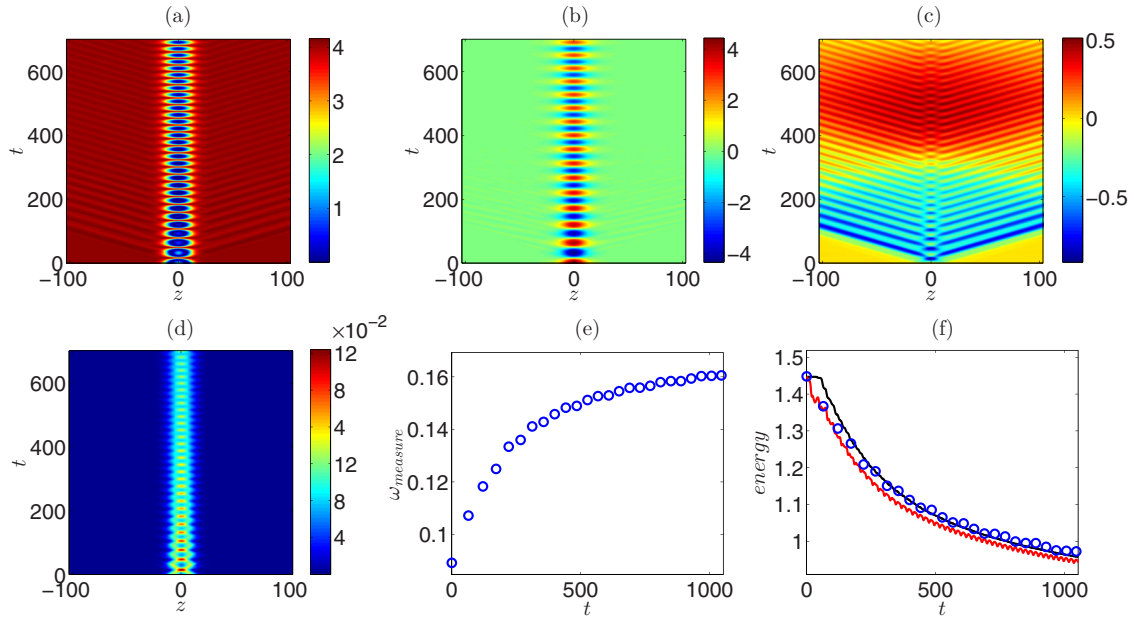


FIG. 1. (Color online) Time evolution of the oscillon with imprinted SG breather parameters, $u = 0.5$ and $v = 0.01$ [Eq. (9)]: (a) The density profile of the two superposed atomic fields, $|\psi_1 + \psi_2|^2$. (b) The spatial distribution of the relative phase, $\phi_1 - \phi_2$. (c) The spatial distribution of the total phase, $\phi_1 + \phi_2$. (d) The density profile of the grand canonical GP energy E . (e) The measured frequency of the oscillon. (f) The computed localized energy of the oscillon: blue circle indicates the energy E_B obtained according to Eq. (12); black line indicates the energy E obtained by integrating Eq. (1); red line indicates the energy H_{SG} obtained by integrating Eq. (6).

and evolve this initial state in accordance with Eqs. (13) and (14).

1. Weak coupling

We first consider the case of a weak-coupling energy $v = 0.01$, and $u = 0.5$ for the initially imprinted SG breather profile. The created oscillon can be easily identified in the pattern of superposition $|\psi_1 + \psi_2|^2$ and in the time-varying spatial distribution of the relative phase $\phi_1 - \phi_2$, as shown in Fig. 1(b). Continuous emission of Bogoliubov sound waves from the oscillon is revealed by the appearance of the wavefronts in Figs. 1(a) and 1(c), which corresponds to the up-chirping of the oscillon frequency as shown in Fig. 1(e). To characterize the evolution of the oscillon, we measure the frequency (period) of the relative phase oscillation shown in Fig. 1(e). To verify the degree of deviation of the oscillon from the SG breather, we compare the energy of the oscillon with those calculated by integrating the GP energy functional (1) and SG Hamiltonian (6) within the region of localization of the oscillon, $-7z_w < z < 7z_w$. As shown in Fig. 1(f), the energies E_B of Eq. (12) obtained from the measured oscillon frequency (blue circle), the GP energy E of Eq. (1) (black line), and the SG Hamiltonian H_{SG} of Eq. (6) (red line) agree closely with each other, implying that the resulting oscillon is almost identical to the SG breather. Furthermore, the red line shows small-amplitude oscillation caused by the coupling of the asymmetric degrees of freedom to the symmetric ones and this suggests that the observed localized energy oscillation is in the context of the oscillon. We also perform the simulations for much smaller couplings, and the oscillation of SG energy and the emission of the Bogoliubov sound are suppressed which suggests that for sufficiently weak coupling

($v \ll 1$) the coupled BECs support long-lived oscillon-type excitations. Studies of both the ϕ^4 and the perturbed SG models have predicted the decay of the oscillon excitation via phonon emission [26–28]. However, in the weakly coupled BEC system we observe a slightly different decaying behavior where the oscillon-type excitations in the asymmetric degrees of freedom lose energy to the symmetric degrees of freedom by emitting Bogoliubov phonons. Unlike the ϕ^4 and SG model, the decay which we observed could only occur in the coupled BECs since the coupled BECs support different degrees of freedom.

2. Strong coupling

In the strong-coupling regime, the relative phase dynamics is beyond the SG description so the dynamical properties of the oscillon are expected to be different from those of the SG breather. To study the oscillon dynamics in the strong-coupling regime, we follow the same simulation procedure in the weakly coupled BECs by imprinting the SG breather onto the ground state. We first consider a stronger coupling energy of $v = 0.5$ and an initially imprinted SG breather of $u = 0.5$. The evolution is shown in Fig. 2, where the imprinted SG breather is unstable and decays into two GP solitons instantly. We see that the two GP grey solitons, which carry the majority of the excitation energy, move towards the boundaries of the coupled condensates. However, we find that the oscillon could remain long lived by increasing u of the initially imprinted SG breather. Now let us consider the same coupling energy but with an otherwise different initial imprinted SG breather of $u = 10$. The time evolution of this initial state is shown in Fig. 3. In Fig. 3(a), the imprinted SG breather emits sound waves initially to reduce its energy and then form the long-lived

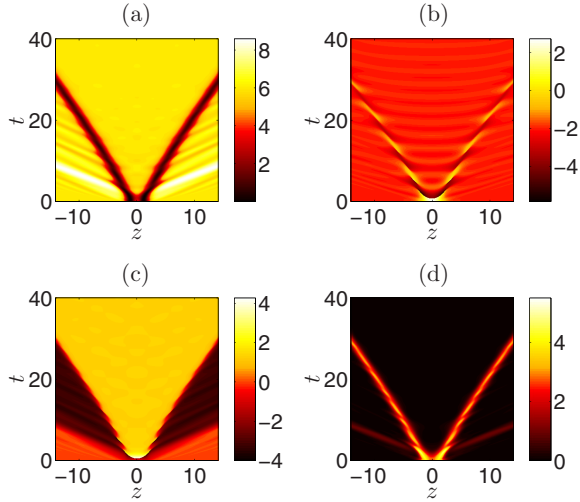


FIG. 2. (Color online) Formation of GP solitons with the imprinted SG breather parameters, $u = 0.5$ and $v = 0.5$ [Eq. (9)]: (a) The density profile of the two superposed atomic fields, $|\psi_1 + \psi_2|^2$. (b) The spatial distribution of the relative phase, $\phi_1 - \phi_2$. (c) The spatial distribution of the total phase, $\phi_1 + \phi_2$. (d) The density profile of the grand canonical GP energy E . Note that the imprinted SG breather is unstable which instantly decays into two GP solitons.

oscillon excitation. In contrast to the oscillon in the SG regime, the oscillon in the strongly coupled BECs exhibits different dynamical behavior: the oscillon only emits sound waves at the beginning and subsequently the total phase manifests localized breathing oscillation as shown in Figs. 3(a) and 3(b). Similar to the weak-coupling case, we also compare the energies of

the oscillon obtained by Eqs. (1), (6), and (12) and find that all these results are noticeably different. We see that the GP energy density [Fig. 3(d)] shows a different behavior from the weak-coupling case [Fig. 1(d)]. The latter exhibits a temporally oscillatory behavior but the former does not. This oscillation implies the energy transfer between the asymmetric degrees of freedom and the symmetric degrees of freedom which also accounts for the emergence of the oscillon in both the total and relative phases. Furthermore, the deviation of GP energy from the breather energy obtained by inserting the measured frequency into Eq. (12) [Fig. 3(e)] implies that the relative dynamics in the present case cannot be properly described by the SG equation. We have also considered a much stronger coupling energy and the result shows similar behavior except a much larger amplitude oscillation in the total phase. The numerical results show the possibility of studying the oscillon-type excitation in the strongly coupled BECs.

3. Phase diagram

From the previous simulations, we conclude that the long-lived oscillon excitation can exist in both weak- and strong-coupling regimes. In general, the stability of the oscillon depends on two parameters, v and u . We notice that u is not directly related to system parameters, but it can be expressed in terms of v and ω_B , the frequency of the initial SG breather. Therefore, it is more practical to characterize the stability of the oscillon as a function of the coupling v and the frequency ω_B of the imprinted breather. We take the relative energy E_r , which is the ratio of remnant GP energy to the GP energy of the imprinted initial state, as a measure of the stability of the oscillon. Here the GP energy of the oscillon

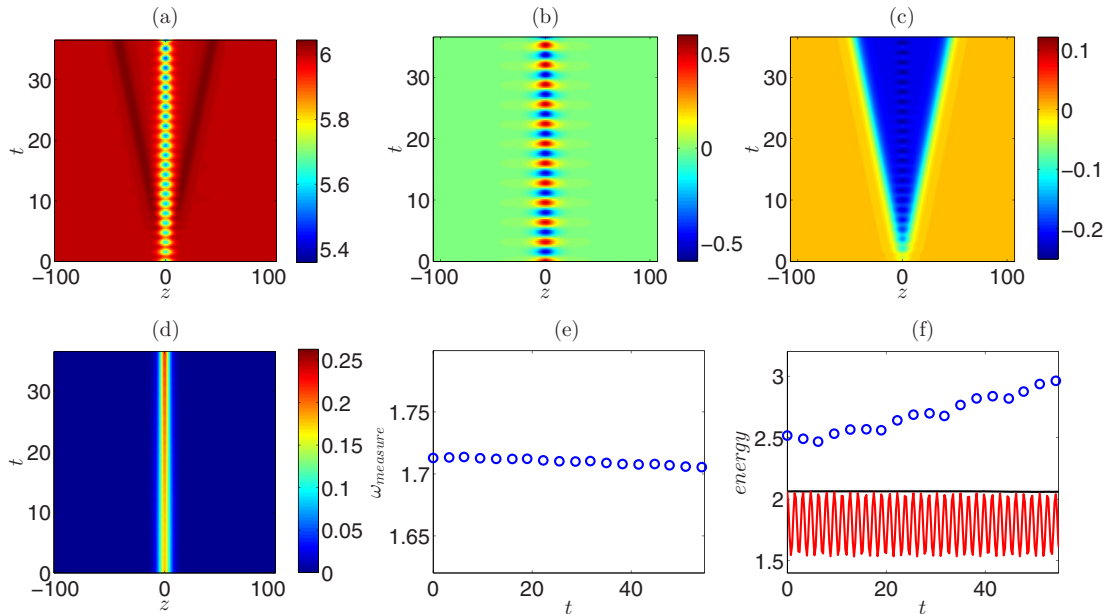


FIG. 3. (Color online) Time evolution of the oscillon with imprinted SG breather parameters, $u = 10$ and $v = 0.5$ [Eq. (9)]: (a) The density profile of the two superposed atomic fields, $|\psi_1 + \psi_2|^2$. (b) The spatial distribution of the relative phase, $\phi_1 - \phi_2$. (c) The spatial distribution of the total phase, $\phi_1 + \phi_2$. (d) The density profile of the grand canonical GP energy E . (e) The measured frequency of the oscillon. (f) The computed localized energy of the oscillon: blue circle indicates the energy E_B obtained according to Eq. (12); black line indicates the energy E obtained by integrating Eq. (1); red line indicates the energy H_{SG} obtained by integrating Eq. (6). The deviation of the red and black lines in (f) indicates that the strongly coupled condensates cannot be described by the SG equation for the relative phase.

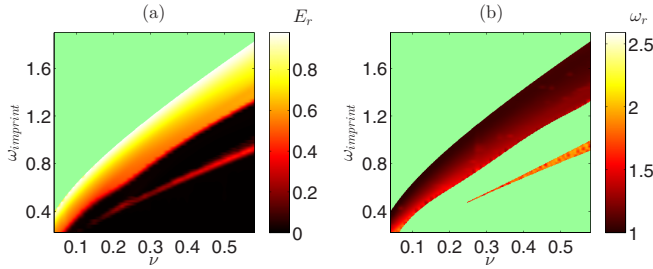


FIG. 4. (Color online) Oscillon stability: (a) The ratio of the remnant GP energy of the oscillon to that of the initial state at $t = 15T_0$ as a function of ω_{imp} and ν (see text). (b) The relative frequency as a function of ω_{imp} and ν . The upper green regions in (a) and (b) indicate where the SG breather initial condition cannot be imprinted. The unstable (black) region in (a) corresponds to the lower green region in (b), as ω_{meas} is undefined.

is evaluated by integrating the energy density over the interval $-7z_w < z < 7z_w$. To avoid the transient effects of the initial phase imprinting, the relative energy is obtained by calculating the ratio of the GP energy at $t = 15T_0$ to that at $t = 0$, where $T_0 = 2\pi/\omega_{\text{imp}}$ is the period of the imprinted SG breather. In the simulation, ν is varied from 0.01 to 0.6, and for each ν , the imprinted frequency ω_{imp} is varied from 0.005 to $\sqrt{4\nu(1+\nu)}$. The limiting value $\sqrt{4\nu(1+\nu)}$ is the maximally possible frequency of the SG breather of Eq. (10) and indicates the boundary beyond which the SG breather cannot be imprinted. Numerically we also find an energy threshold for stability given by $E_r \sim 0.4$, i.e., the oscillon is unstable if $0 < E_r \lesssim 0.4$ and stable if $0.4 \lesssim E_r \leq 1$.

The results are shown in Fig. 4(a), where we see that the oscillon as the remnant of the imprinted SG breather is always long lived ($E_r \sim 1$) as long as $\nu < 0.04$. In Fig. 4(a), the upper green area marks the forbidden domain where no SG breather can be phase imprinted and the black area indicates the domain where the imprinted SG breather would instantly decay into two GP solitons as shown in Fig. 2. Moreover, we observe that the oscillon energy loss is accompanied by an up-chirping of its oscillation frequency with time. Hence, the frequency chirping of the oscillon can also serve as a measure of stability. To this end, we consider the relative frequency $\omega_r = \bar{\omega}_{\text{meas}}/\omega_{\text{imp}}$, where $\bar{\omega}_{\text{meas}}$ is defined as the mean frequency of the oscillon averaged over the time interval $10T_0 \leq t \leq 15T_0$; this interval includes several oscillations, while being much shorter than the chirp time scale. The results of the frequency chirping are shown in Fig. 4(b). Besides the green area in the energy diagram, there are two stable domains having relative energy above the threshold. The upper stable domain in the energy diagram shows a lower chirping rate frequency compared to that of the lower (narrow) stable domain. This suggests that the energy decay is stronger in the lower stable domain than in the upper stable domain. We also observe that, while increasing the frequency of the imprinted SG breather at a given coupling energy, the two grey GP solitons originating from the decay of the imprinted SG breather, which are visible in Figs. 2(a) and 2(c), would gradually speed up in the black area of the energy diagram. The decay into two grey GP solitons arises in the lower stability region as well, yet the emitted solitons acquire a speed very close to that of Bogoliubov sound,

indicating that the solitons are very unstable in this domain. Note that in the upper stable domain, there are no grey solitons, but instead two outgoing small density bumps appear when the oscillon is stabilized as shown in Fig. 3.

We note that since the dynamical properties of the oscillon in a strong-coupling regime are different from those of the SG breather, the frequency of the imprinted SG breather may not serve as the relevant parameter to describe the stability of an oscillon in the strong-coupling regime, which leads to the appearance of the bifurcated stable domain in the strong-coupling regime (starting around $\nu \approx 0.2$ in Fig. 4).

We have shown how the oscillon originating from a SG breather loses its energy in both weak- and strong-coupling cases. The influence of external perturbations upon the dynamics of topology-protected excitations [33], so to speak, is broadly analogous to the influence of integrability breaking on oscillons and solitons [34,35], namely, that the breakdown of strict integrability couples the excitation to additional degrees of freedom that can extract its energy. Intriguingly, we find that the formation of oscillons could be related to the collision of Josephson vortices, and in next section we shall address such a possibility.

IV. FORMATION OF AN OSCILLON

Since Josephson vortices are topologically stable excitations of the coupled BEC system, they can spontaneously form during the BEC phase transition via the Kibble-Zurek mechanism [23,36] and may then collide to form an oscillon. A Josephson vortex pair could also be phase imprinted and then allowed to collide. In this section we study the Josephson vortex collision process as a basic prototype of oscillon formation.

A. Collision of Josephson vortices

We simulate the collision of two Josephson vortices of opposite handedness, namely, kink and antikink, which provides a possibility of generating an oscillon for Eq. (13). We recall that the static Josephson vortices in the linearly coupled BECs exist when $\tilde{v}/\mu < 1/3$, and closed form expressions are known from Ref. [18]. To obtain a solution for moving Josephson vortices, we assume solutions propagating with constant velocity and solve the resulting coupled GPEs numerically, increasing the velocity in small steps starting from zero [22]. The initial state for the time-dependent simulation is made up of two countermoving Josephson vortices with speed $|v| = 0.1$, initially located at both sides with equal distance from the origin. As can be seen from Fig. 5, the head-on collision of two Josephson vortices takes place at the origin. Remarkably, the two Josephson vortices do not annihilate each other but bind together to form an oscillon excitation after the collision. As soon as the oscillon is formed, it continuously emits Bogoliubov sound waves. Since the coupling is very weak, it is expected that the relative phase dynamics is essentially governed by the SG equation, and the oscillon emerging from the collision of two Josephson vortices (SG kinks) appears very close to a SG breather, as the one depicted in Fig. 1. As shown in Fig. 5(a), the frequency of the

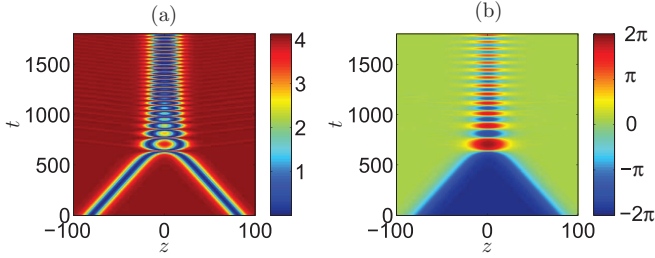


FIG. 5. (Color online) Collision of two Josephson vortices ($\nu = 0.005$): (a) The density profile of the two superposed atomic fields, $|\psi_1 + \psi_2|^2$. (b) The spatial distribution of the relative phase, $\phi_1 - \phi_2$. The two counter-moving Josephson vortices with velocities $v = \pm 0.1$ collide at the instant $t = 800$ forming an oscillon. As shown in (a), the quasibreather continuously radiates Bogoliubov sound waves to the background superfluid, causing an up-chirp of the oscillon's oscillation frequency.

oscillon increases with time. According to Eq. (12), increasing ω_B will lower the value of E_B , implying that the oscillon in Fig. 5(a) gradually loses its energy. This decay is due to the fact that the relative phase ϕ_a can couple to the other degrees of freedom in the GP energy, namely, the total phase ϕ_S and density ρ . Although the oscillon is not an exact SG breather and undergoes damping, it has a very long lifetime compared to its breathing period, suggesting that oscillon excitations in linearly coupled BECs may be observable in BEC experiments.

B. Constraints for phase imprinting

We have systematically studied the oscillon in the coupled BECs at different regimes of coupling strength. A possible way to realize the oscillon is to phase imprint the relative phase profile by shining a Gaussian laser beam onto the coupled BEC system, so that the Stark effect generated by the laser can cause a controllable position-dependent phase difference between the two BECs. To create the required relative phase profile, the laser beam should be focused between the two BECs and the focusing point should sit slightly away from the centerline between the two BECs. Assuming that the phases imprinted on the two BECs take the form

$$\phi_1^i = A \exp[-z^2/\kappa^2], \quad \phi_2^i = \epsilon A \exp[-z^2/\kappa^2], \quad (16)$$

where κ is the width of the Gaussian beam, α is the geometric factor due to the departure of focal point from the centerline between the two condensates, and A is proportional to the product of laser intensity and time duration of the exposure. As a consequence, the relative phase is given by $\Delta\phi = (1 - \epsilon)A \exp[-z^2/\kappa^2]$. Matching the amplitude and width of $\Delta\phi$ to those of the SG breather given by Eq. (9), the width κ and the amplitude A can be determined after some algebra as

$$\kappa^2 = \frac{z_w^2}{\ln\left(\tan^{-1}\frac{\sqrt{1+v}}{u}\right) - \ln\left(\tan\frac{\sqrt{1+v}}{2u}\right)}, \quad (17)$$

$$A = \frac{4}{1 - \epsilon} \tan^{-1} \frac{\sqrt{1+v}}{u}, \quad (18)$$

where z_w is the FWHM of the SG breather defined previously. Note that the parameter range of the imprinted Gaussian

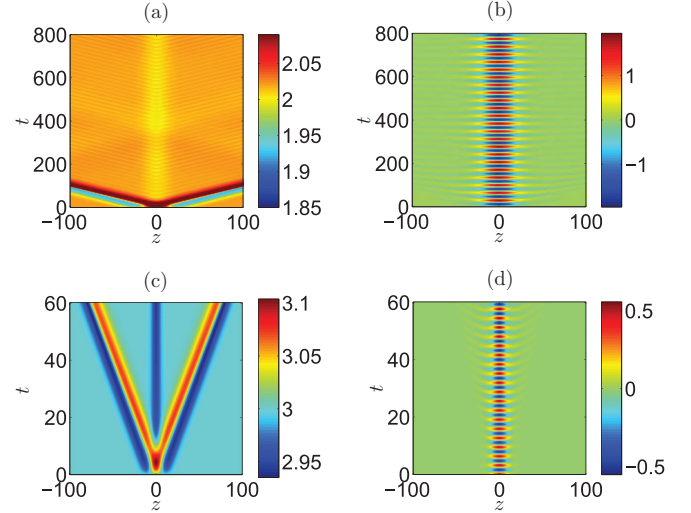


FIG. 6. (Color online) Dynamics following a Gaussian phase imprint as described in the text. Panels (a) and (c) show the density profile of the superposition $|\psi_1 + \psi_2|^2$, and (b) and (d) show the relative phase $\phi_1 - \phi_2$ for two different sets of initial parameters: $u = 2$, $\nu = 0.01$, $\epsilon = 0.2$ [(a) and (b)] and $u = 10$, $\nu = 0.5$, $\epsilon = 0.2$ [(c) and (d)]. In both cases a long-lived breather is created as seen in the relative phase.

phase is limited since Eq. (17) becomes imaginary when $\tan(\sqrt{1+v}/2u) > \tan^{-1}(\sqrt{1+v}/u)$.

To demonstrate that the aforementioned method is practical, we simulate Eq. (13) by phase imprinting the Gaussian phase profile with $(\nu, \epsilon, u) = (0.01, 0.2, 2)$ and $(0.5, 0.2, 10)$ and the width κ and the amplitude A are given according to Eqs. (17) and (18). Note that according to the assumption in Eq. (16), a nonzero total phase will also be imprinted, which causes disturbance in the total density. As shown in Fig. 6, this disturbance is detectable only in the atomic interference pattern Figs. 6(a) and 6(c) despite the creation of an oscillon excitation in the relative phase [Figs. 6(b) and 6(d)].

V. CONCLUSIONS

We have theoretically studied the dynamics of an oscillon in the relative phase of two linearly coupled Bose-Einstein condensates. The stability of the oscillon has been examined over broad ranges of coupling energy and imprinted SG breather frequency. In the weak-coupling limit, the system exhibits SG dynamics predominantly, and thus an oscillon forms a long-lived metastable excitation, despite gradually losing energy to Bogoliubov phonons. In the strong-coupling regime, the system dynamics is no longer governed by the SG equation for the relative phase due to the increasingly prominent interplay between the symmetric and asymmetric degrees of freedom. A systematic study of parameter space reveals large regions where the lifetime of the oscillon exceeds its period by several orders of magnitude. The experimental realization of oscillons may enable the possibility of using Bose-Einstein condensates as an analog model to simulate and characterize oscillon formation in the dynamics of the early universe.

ACKNOWLEDGMENTS

We are indebted to Sophie Shamailov for the provision of numerical code for generating moving Josephson vortices used for Sec. IV A and for useful comments on the manuscript. A.B. was supported by a Rutherford Discovery Fellowship administered by the Royal Society of New Zealand. O.F. was

supported by the Marsden Fund (Project No. MAU 1205), administrated by the Royal Society of New Zealand. S.W.S., S.C.G., and I.K.L. were supported by the Ministry of Science and Technology, Taiwan (Grant No. MOST 103-2112-M-018-002-MY3). S.C.G. was also supported by the National Center for Theoretical Sciences, Taiwan.

-
- [1] I. Bogolyubskii and V. Makhankov, *JETP Lett.* **24**, 12 (1976).
 [2] M. Gleiser, *Phys. Rev. D* **49**, 2978 (1994).
 [3] T. Vachaspati, *Kinks and Domain Walls: An Introduction to Classical and Quantum Solitons* (Cambridge University Press, Cambridge, UK, 2006).
 [4] E. J. Copeland, M. Gleiser, and H.-R. Müller, *Phys. Rev. D* **52**, 1920 (1995).
 [5] M. A. Amin, R. Easther, H. Finkel, R. Flauger, and M. P. Hertzberg, *Phys. Rev. Lett.* **108**, 241302 (2012).
 [6] M. B. Hindmarsh and T. W. B. Kibble, *Rep. Prog. Phys.* **58**, 477 (1995).
 [7] M. Ablowitz, D. Kaup, A. Newell, and H. Segur, *Phys. Rev. Lett.* **30**, 1262 (1973).
 [8] N. N. Akhmediev, V. M. Eleonskii, and N. E. Kulagin, *Theor. Math. Phys.* **72**, 809 (1987).
 [9] S. Flach and C. Willis, *Phys. Rep.* **295**, 181 (1998).
 [10] E. Bour, *J. École Imperiale Polytech.* **19**, 1 (1862).
 [11] J. Frenkel and T. Kontorova, *J. Phys. (Moscow)* **1**, 137 (1939).
 [12] T. Dauxois and M. Peyrard, *Physics of Solitons* (Cambridge University Press, Cambridge, UK, 2006).
 [13] M. Peyrard and D. K. Campbell, *Physica D (Amsterdam, Neth.)* **9**, 33 (1983).
 [14] F. K. Abdullaev, A. Gammal, B. A. Malomed, and L. Tomio, *Phys. Rev. A* **87**, 063621 (2013).
 [15] V. Gritsev, A. Polkovnikov, and E. Demler, *Phys. Rev. B* **75**, 174511 (2007).
 [16] C. Neuenhahn, A. Polkovnikov, and F. Marquardt, *Phys. Rev. Lett.* **109**, 085304 (2012).
 [17] B. Opanchuk, R. Polkinghorne, O. Fialko, J. Brand, and P. D. Drummond, *Ann. Phys. (NY)* **525**, 866 (2013).
 [18] V. A. Kurov and A. B. Kuklov, *Phys. Rev. A* **71**, 011601 (2005).
 [19] V. M. Kurov and A. B. Kuklov, *Phys. Rev. A* **73**, 013627 (2006).
 [20] J. Brand, T. J. Haigh, and U. Zülicke, *Phys. Rev. A* **80**, 011602(R) (2009).
 [21] M. I. Qadir, H. Susanto, and P. C. Matthews, *J. Phys. B: At. Mol. Opt. Phys.* **45**, 035004 (2012).
 [22] S. S. Shamailov and J. Brand (unpublished).
 [23] S.-W. Su, S.-C. Gou, A. Bradley, O. Fialko, and J. Brand, *Phys. Rev. Lett.* **110**, 215302 (2013).
 [24] V. Ambegaokar, U. Eckern, and G. Schön, *Phys. Rev. Lett.* **48**, 1745 (1982).
 [25] U. Eckern, G. Schön, and V. Ambegaokar, *Phys. Rev. B* **30**, 6419 (1984).
 [26] H. Segur and M. D. Kruskal, *Phys. Rev. Lett.* **58**, 747 (1987).
 [27] J. P. Boyd, *Nonlinearity* **3**, 177 (1990).
 [28] J. Denzler, *Commun. Math. Phys.* **158**, 397 (1993).
 [29] P. S. Lomdahl, O. H. Olsen, and M. R. Samuelsen, *Phys. Rev. A* **29**, 350 (1984).
 [30] A. A. Penckwitt, R. J. Ballagh, and C. W. Gardiner, *Phys. Rev. Lett.* **89**, 260402 (2002).
 [31] M. Tsubota, K. Kasamatsu, and M. Ueda, *Phys. Rev. A* **65**, 023603 (2002).
 [32] T. P. Billam, M. T. Reeves, B. P. Anderson, and A. S. Bradley, *Phys. Rev. Lett.* **112**, 145301 (2014).
 [33] S. J. Rooney, A. S. Bradley, and P. B. Blakie, *Phys. Rev. A* **81**, 023630 (2010).
 [34] A. D. Martin and J. Ruostekoski, *New J. Phys.* **12**, 055018 (2010).
 [35] N. G. Parker, N. P. Proukakis, and C. S. Adams, *Phys. Rev. A* **81**, 033606 (2010).
 [36] A. Das, J. Sabbatini, and H. W. Zurek, *Sci. Rep.* **2**, 352 (2012).